NASA
Technical Memorandum 103109

AVSCOM
Technical Report 89-C-022

Dynamics of Multistage Gear Transmission With Effects of Gearbox Vibrations

F.K. Choy and Y.K. Tu
The University of Akron
Akron, Ohio

and

J.J. Zakrajsek and D.P. Townsend
Lewis Research Center
Cleveland, Ohio

Prepared for the
CSME Mechanical Engineering Forum 1990
sponsored by the Canadian Society of Mechanical Engineers
Toronto, Canada, June 3-9, 1990

NASA

US ARMY
AVIATION
SYSTEMS COMMAND
AVIATION R&T ACTIVITY

ERRATA

NASA Technical Memorandum 103109

DYNAMICS OF MULTISTAGE GEAR TRANSMISSION WITH EFFECTS OF GEARBOX VIBRATIONS

F.K. Choy, Y.K. Tu,
J.J. Zakrajsek, and D.P. Townsend

June 1990

Cover and report documentation page: The AVSCOM Technical Report number should be 89-C-022.

DYNAMICS OF MULTISTAGE GEAR TRANSMISSION WITH EFFECTS OF GEARBOX VIBRATIONS

F.K. Choy and Y.K. Tu
Department of Mechanical Engineering
The University of Akron
Akron, Ohio 44325

J.J. Zakrajsek and D.P. Townsend
National Aeronautics and Space Administration
Lewis Research Center
Cleveland, Ohio 44135

SUMMARY

This paper presents a comprehensive approach in analyzing the dynamic behavior of multistage gear transmission systems with the effects of gearbox induced vibrations and mass imbalances of the rotor. The modal method, with undamped frequencies and planar mode shapes, is used to reduce the degrees of freedom of the gear system for time-transient dynamic analysis. Both the lateral and torsional vibration modes of each rotor-bearing-gear stage as well as the interstage vibrational characteristics are coupled together through localized gear mesh tooth interactions. In addition, gearbox vibrations are also coupled to the rotor-bearing-gear system dynamics through bearing support forces between the rotor and the gearbox. Transient and steady state dynamics of lateral and torsional vibrations of the geared system are examined in both time and frequency domains to develop interpretations of the overall modal dynamic characteristics under various operating conditions. A typical three-stage geared system is used as an example. Effects of mass imbalance and gearbox vibrations on the system dynamic behavior are presented in terms of modal excitation functions for both lateral and torsional vibrations. Operational characteristics and conclusions are drawn from the results presented.

INTRODUCTION

In the continuous search for the improvements in operational life, efficiency, maintainability, and reliability in gear transmission systems, one of the major objectives in design improvement is the reduction of noise and vibration in the transmission system. Two main streams of work have been carried out in the areas of noise and vibration reduction; namely (1) the localized gear-tooth stress/thermal effects during gear interactions [Cornell 1981, Lin 1988, Boyd 1987, Savage 1986], and (2) the overall global dynamic behavior [August 1986, Choy 1989, David 1987, 1988, Mitchell 1985] of the transmission systems.

The work presented in this paper is the development and application of a comprehensive approach in simulating the overall dynamics of a multistage rotor-bearing-gear system. The modal method is applied to reduce the degrees of freedom of the global system of equations. Various operational characteristics are simulated in the analysis, such as

(1) Multistage rotor-gear configuration
(2) The coupling of gearbox vibrations
(3) The effects of rotor mass-imbalance and shaft bow
(4) The effects of inertia-gyroscopic moments
(5) The effects of nonlinear gear mesh stiffnesses
(6) Variable shaft geometry and bearing support characteristics

The modal equations of motion are solved to evaluate system acceleration at each time step. A self-adaptive variable time-stepping integration technique [Choy 1987, 1988, 1989] is used to calculate the transient dynamics of the system. A typical three-stage rotor-bearing-gear system is used as an example in this analysis. Results are presented in both time and frequency domains to develop a vibration signature analysis of the system.

NOMENCLATURE

$A_i(t)$	modal function of the i^{th} mode in x-direction
$A_{ti}(t)$	modal function of the i^{th} mode in Θ-direction
$B_i(t)$	modal function of the i^{th} mode in y-direction
$[C_T]$	torsional damping matrix
$[C_{xx}],[C_{xy}]$	bearing direct and cross-coupling damping matrices
$[C_{yx}],[C_{yy}]$	
$F_{Gt}(t)$	gear mesh torque
$F_{Gx}(t),F_{Gy}(t)$	gear mesh force in x- and y-directions
$F_t(t)$	external excitation moment
$F_x(t),F_y(t)$	external excitation forces
$[G_x],[G_y]$	gyroscopic-inertia matrix
$[I]$	identity matrix
$[J]$	rotational mass moment of inertia matrix
K_s	shaft stiffness matrix
$[K_T]$	torsional stiffness matrix
K_{tki}	gear mesh stiffness between i^{th} and k^{th} rotor
$[K_{xx}],[K_{xy}]$	bearing direct and cross-coupling damping matrix
$[K_{yx}],[K_{yy}]$	
$[M]$	mass-inertia matrix

R_{ci}	radius of gear in the i^{th} rotor
T_F	gear generated torque
X_{ci}, Y_{ci}	gear displacements in x- and y-directions of the i^{th} rotor
X_F, Y_F	gear forces in x- and y-directions
α_{ki}	angle of tooth mesh between k^{th} and i^{th} rotor
$[\Lambda^2]$, $[\Lambda_t^2]$	lateral and torsional eigenvalue diagonal matrices
$[\Phi]_k, [\Phi_t]_k$	lateral and torsional orthonormal eigenvalue diagonal matrices of the k^{th} rotor

DEVELOPMENT OF EQUATIONS OF MOTION

The equations of motion for a single stage multimass rotor-bearing-gear system with the effects of gearbox motion induced vibrations at the bearing supports, rotor inertia and gyroscopic effects, and excitations from rotor mass imbalance and residual runouts can be written in matrix form [Choy 1987, 1989] for the X-Y plane as

$$[M]\{\ddot{X}\} + [G_x]\{\dot{X}\} + [C_{xx}]\{\dot{X} - \dot{X}_b\} + [C_{xy}]\{\dot{Y} - \dot{Y}_b\} + [G_y]\{Y\} + [K_{xx} + K_s]\{X\} - [K_{xx}]\{X_b\} + [K_{xy}]\{Y - Y_b\} = \{F_x(t)\} + \{F_{Gx}(t)\} \quad (1)$$

and in the Y-Z plane as

$$[M]\{\ddot{Y}\} - [G_x]\{\dot{Y}\} + [C_{yx}]\{\dot{X} - \dot{X}_b\} + [C_{yy}]\{\dot{Y} - \dot{Y}_b\} - [G_y]\{Y\} + [K_{yy} + K_s]\{Y\} - [K_{yy}\{Y_b\} + [K_{yx}]\{Y - Y_b\} = \{F_y(t)\} + \{F_{Gy}(t)\} \quad (2)$$

Here F_x and F_y are force excitations from the effects of mass imbalance, shaft residual bow and bearing support base motion in both X- and Y-directions. The X and Y gear mesh forces, F_{Gx} and F_{Gy}, are induced from the gear teeth interaction with other coupled gear stages. The bearing forces are evaluated through the relative motion between the rotor $\{X\}$, $\{Y\}$ and the gearbox $\{X_b\}$, $\{Y_b\}$ at the bearing locations [Choy 1987]. The mass-inertia and gyroscopic effects are incorporated in the mass matrix [M] and the gyroscopic matrices $[G_x]$ and $[G_y]$. The coupled torsional equations of motion for the single rotor-bearing-gear system can be written as follows:

$$[J]\{\ddot{\Theta}\} + [C_T]\{\dot{\Theta}\} + [K_T]\{\Theta\} = \{F_T(t)\} + \{F_{Gt}(t)\} \quad (3)$$

In equation (3), $\{F_T(t)\}$ represents the externally applied torque and $\{F_{Gt}(t)\}$ represents the gear mesh induced moment. Note that equations (1) to (3) repeat for each single gear/rotor stage. The gear mesh forces couple the force equations of each stage to each other as well as the torsional equations to the lateral equations [Choy 1989, Cornell 1981, David 1987, 1988]. The coupling

relationships between the torsional and the lateral vibrations and the dynamics of each individual gear/rotor stage are derived in the next section.

COUPLING IN GEAR MESHES

The torsional and lateral vibrations of a single, individual rotor and the dynamic relationships between each gear stage are coupled through the nonlinear interactions in the gear mesh. Gear mesh forces and moments are evaluated as functions of relative motion and rotation between two meshing gears and the corresponding gear mesh stiffnesses. These gear mesh stiffnesses vary in a repeating nonlinear pattern [August 1986, Cornell 1981, Savage 1986] with each tooth pass engagement period and can be represented by a high order polynomial [Cornell 1981, Boyd 1987]. The periodic nature of such nonlinear mesh stiffnesses can also act as a source of steady state excitation to the gear system. With the coordinate system as shown in figure 1, the following gear mesh coupling equations can be established by equating force and moment [Choy 1989]. For the k^{th} stage gear of the system, summing force in the X-direction results in the following:

$$X_F = \sum_{i=1, i\neq r}^{n} K_{tki}[-R_{ci}\Theta_{ci} + R_{ck}\Theta_{ck} + (X_{ci} - Y_{ck})\cos\alpha_{ki} + (Y_{ci} - Y_{ck})\sin\alpha_{ki}]\cos\alpha_{ki} \qquad (4)$$

Summing force in the Y-direction results in

$$Y_F = \sum_{i=1, i\neq k}^{n} K_{tki}[-R_{ci}\Theta_{ck} - R_{ck}\Theta_{ck} + (X_{ci} - X_{ck})\cos\alpha_{ki} + (Y_{ci} - Y_{ck})\sin\alpha_{ki}]\sin\alpha_{ki} \qquad (5)$$

Summing moment in the Z-direction results in

$$T_F = \sum_{i=1, i\neq k}^{n} R_{ck}[K_{tki}(-R_{ci}\Theta_{ci} - R_{ck}\Theta_{ck})] \qquad (6)$$

where n is the number of stages in the system.

MODAL ANALYSIS

To reduce the computational effort, the number of degrees of freedom of the system of equations is reduced through modal transformation. Orthonormal modes for each individual rotor-bearing stage are obtained by solving the uncoupled system homogeneous characteristic equations. With the modal expansion approach [Choy 1987, 1988, 1989], the motion of the system can be expressed as

$$\{X\} = \sum_{i=1}^{m} A_i \{\phi_i\} \tag{7}$$

$$\{Y\} = \sum_{i=1}^{m} B_i \{\phi_i\} \tag{8}$$

$$\{\Theta\} = \sum_{i=1}^{m} At_i \{\phi_{ti}\} \tag{9}$$

where m is the number of modes used. The orthogonality conditions of the modes can be expressed as

$$[\Phi]^T[K][\Phi] = [\Lambda^2] \tag{10}$$

$$[\Phi_t]^T[K_t][\Phi_t] = [\Lambda_t^2] \tag{11}$$

$$[\Phi]^T[M][\Phi] = [\Phi_t]^T[J][\Phi_t] = [I] \tag{12}$$

With the modal expansion and the orthogonality conditions, the modal equations of motion [Choy 1989] can be written as follows:

X-Z equation

$$\{\ddot{A}\} + [\Phi]^T[G_x][\Phi]\{\dot{A}\} + [\phi]^T[C_{xx}][\Phi]\{\dot{A}\} + [\Phi]^T[C_{xy}][\Phi]\{\dot{B}\} + [\Phi]^T[G_y][\Phi]\{B\}$$
$$+ [\Lambda^2]\{A\} + [\Phi]^T[K_{xy}][\Phi]\{B\} = [\Phi]^T\{F_x(t) + F_{Gx}(t)\} \tag{13}$$

Y-Z equation

$$\{\ddot{B}\} - [\Phi]^T[G_x][\Phi]\{\dot{B}\} + [\Phi]^T[C_{yx}][\Phi]\{\dot{A}\} + [\Phi]^T[C_{yy}][\Phi]\{\dot{B}\} - [\Phi]^T[G_y][\Phi]\{A\}$$
$$+ [\Lambda^2]\{B\} + [\Phi]^T[K_{yx}][\Phi]\{A\} = [\Phi]^T\{F_y(t) + F_{Gy}(t)\} \tag{14}$$

Θ-equation

$$\{\ddot{A}_t\} + [\Phi_t]^T[C_T][\Phi_t]\{\dot{A}_t\} + [\Lambda_t^2]\{A_t\} = [\Phi_t]^T\{F_t(t) + F_{Gt}(t)\} \tag{15}$$

The gear mesh forces and moment can also be expressed in the modal form, for the k^{th} stage, as follows:

$$[\Phi]_k^T\{X_F\} = \sum_{j=1}^{m} \phi_{kjl} \left\{ \sum_{i=1, i\neq k}^{n} K_{tki}[-R_{ci}\theta_{ci} - R_{ck}\theta_{ck} + (x_{ci} - x_{ck})\cos\alpha_{ki} + (y_{ci} - y_{ck})\sin\alpha_{ki}]\cos\alpha_{ki} \right\} \quad (16)$$

$$[\Phi]_k^T\{Y_F\} = \sum_{j=1}^{m} \phi_{kjl} \left\{ \sum_{i=1, 1\neq k}^{n} K_{tki}[-R_{ci}\theta_{ci} - R_{ck}\theta_{ck} + (x_{ci} - x_{ck})\cos\alpha_{ki} + (y_{ci} - y_{ck})\sin\alpha_{ki} \right\} \quad (17)$$

$$[\Phi]_k^T\{T_F\} = \sum_{j=1}^{m} \phi_{kjl} \left\{ \sum_{1=1, 1\neq k}^{n} R_{ck}[K_{tki}(-R_{ci}\theta_{ci} - R_{ck}\theta_{ck})] \right\} \quad (18)$$

where K is the stage number, j is the mode number, and l is the station location of the gear mesh.

SOLUTION PROCEDURE

Rearrange the modal equations of motion developed in equations (13) to (15) into the following:

X-equation

$$\{\ddot{A}\} = -[\Phi]^T[G_x][\Phi]\{\dot{A}\} - [\Phi]^T[C_{xx}][\Phi]\{\dot{A}\} - [\Phi]^T[C_{xy}][\Phi]\{\dot{B}\} - [\Phi]^T[G_y][\Phi]\{B\} - [\Lambda^2]\{A\} - [\Phi]^T[K_{xy}][\Phi]\{B\} + [\Phi]^T\{F_x(t) + F_{Gx}(t)\} \quad (19)$$

Y-equation

$$\{\ddot{B}\} = [\Phi]^T[G_x][\Phi]\{\dot{B}\} - [\Phi]^T[C_{yx}][\Phi]\{\dot{A}\} - [\Phi]^T[C_{yy}][\Phi]\{\dot{B}\} + [\Phi]^T[G_y][\Phi]\{B\} - [\Lambda^2]\{B\} - [\Phi]^T[K_{yx}][\Phi]\{A\} + [\Phi]^T\{F_y(t) + F_{Gy}(t)\} \quad (20)$$

Θ-equation

$$\{\ddot{A}_t\} = -[\Phi_T]^T[C_T][\Phi_t]\{\dot{A}_t\} - [\Lambda_t^2]\{\dot{A}_t\}[\Phi_t]^T + \{F_t(t) + F_{Gt}(t)\} \quad (21)$$

A variable time stepping Newmark-Beta integration scheme evaluates the modal velocity and displacement at each time interval. In turn, equations (7) to (9) transform the modal displacements into absolute relative displacements in fixed coordinates. The gear mesh forces can be evaluated by the relative motion between the gear teeth using the nonlinear stiffnesses developed for the gear mesh interaction. The effects of gearbox vibration can be calculated as nonlinear bearing forces through the relative vibration between the gearbox and

the shaft at the bearing locations. Since the gearbox and the shaft both are vibrating independently, a separate transient integration scheme is required for each system at every time step before the coupling of bearing forces.

DISCUSSION OF RESULTS

To demonstrate the application of the discussed analytical method, a typical three-stage gear transmission given in figure 2 is used as an example. All three gear stages have an identical 36-tooth gear and a mesh contact ratio of 1.6. Stage I of the system is the driver with a rotational speed of 3000 rpm and an input torque of 2.25 kN-m. Both stages I and II are supported by three bearings while stage III only has two bearing supports. The first two bearings in stages I to III and the third bearings in stages I and II are identical. The rotor in stages I and II is 2.4 in. (6.1 cm) in diameter and has a length of 40 in. (101 cm) and 30 in. (76 cm), respectively. The rotor in stage III is smaller with a diameter of 1.4 in. (3.5 cm) and a length of 20 in. (51 cm). For demonstration purposes, the first three basic modes of the system are used in the modal analysis. Table I provides the information on the modal frequencies of the system in both lateral and torsional directions. Figures 3 and 4 give the orthonormal mode shapes of the first two basic torsional and lateral modes for all three rotor stages. Note that the general form of mode shapes in stage I is more like a mirror image compacted to those of stages II and III which are generally identical. This is due to the fact that a nominal support stiffness is assumed at the gear locations, which produce a substantial difference on the vibratory modes of each rotor stage.

In order to investigate the effects of gearbox vibrations and rotor mass imbalance, results from four major cases of external excitations are examined in this study, namely

Case 1. - No gearbox vibration and small mass imbalance
Case 2. - Gearbox vibration and small mass imbalance
Case 3. - No gearbox vibration and large mass imbalance
Case 4. - Gearbox vibration and large mass imbalance

The gearbox vibrational effects are assumed to be a steady state vibration motion of 1200 Hz at the bearing supports. Vibrational orbits of all three rotor stages at the gear location for all four cases, respectively, are given in figures 5 to 7. Note that the vibratory characteristics of stage I is more influenced by mass imbalance while those of stages II and III are affected by motion of the gearbox through the bearing supports. As we can see from figure 5(b), the effects of bearing support motion to stage I gear vibrational orbits are quite small. This is due to the fact that the rotor of stage I is substantially more flexible than the other two rotors and less influence from the bearing can be effectively converted to the system. In addition, although similar mass imbalances are applied to each rotor stage, vibratory orbits in stages II and III are smaller in amplitude because of their larger rotor stiffnesses.

Figures 8 to 10 depict the first modal component of rotor stages I to III, respectively. Figure 8 shows the effects of the four external excitations on the first modal vibratory component of stage I in both time and frequency domains. Note that figures 8(a) and (b) show that, for small imbalance with no gearbox motion, only very small vibratory motion will result except for the

dc component at zero frequency. Figures 8(c) and (d) represent the first mode rotor vibrations resulting from gearbox motion. Note that the major component occurs at 1200 Hz (input vibratory frequency at the bearing supports) with a minor component at 115 Hz (first natural frequency of stage I). Figures 8(e) and (f) show the effect of mass imbalance, which results in a large component at the rotor speed of 50 Hz and a smaller component at the first mode of 115 Hz. Figures 8(g) and (h) produce the combined effect of gearbox vibration and imbalance on rotor first mode vibrations. By examining the relative amplitudes of the major components, rotor speed, and gearbox vibration frequency, with their corresponding input excitation magnitude, the sensitivity of the rotor to imbalance and gearbox vibration can be determined. Similar conclusions can be arrived in figures 9 and 10 for stages II and III, except that the effects of mass imbalance on first mode vibration is significantly reduced. As we can see in figures 9(g) and (h) and 10(g) and (h), when both excitations are present, the gearbox motion has a much more dominating affect in rotor vibration for stages II and III as compared to stage I. Figures 11 to 13 show the vibration of the second mode component for the three rotor stages, respectively. Note in figure 11, for stage I the second mode vibrational characteristics are very similar to those of the first mode. However, magnitudes of the second mode are approximately 20 percent of those of the first mode. This is because the first mode in the first stage is more easily excited by the imbalances and gear forces acting at the gear location. Further examinations of figures 12 and 13 show that the second mode is more excited than the first mode in the second and third rotor stages. A more detailed study of figures 3 and 4 reveals that the second mode in stages II and III is very similar to the shape of the first mode in stage I, which is the first fundamental bending mode of the overhung rotor system. In addition, from figures 8 to 13, it was found that none of the torsional vibratory frequencies and gear meshing frequencies are excited in the lateral rotor vibration of the system.

Figure 14 depicts the gear mesh forces with effects of both imbalance and gearbox motion excitations. Note that the major component of these forces is the dc component at zero frequency which is due to the constant applied torque. The other sizable force component is at the tooth meshing frequency of 1800 Hz. The higher ac component which results in higher meshing frequency component between gears I and III, is because of the lower rotational stiffness in the stage III rotor. This can also be observed by the higher dc (zero frequency component) in stage III compared to stage II, as shown in figures 15 and 16. Only a very small force component can be observed at the gear mesh frequency (1800 Hz) and first mode frequencies of stage I (355 Hz), stage II (550 Hz), and stage III (280 Hz). Again figures 15 and 16 outline the modal rotational vibration characteristics of all rotor stages with both excitations. Note in figure 15 that other than the zero frequency component, the other sizable vibration is at its own rotational modal frequency (i.e., 355 Hz at stage I, 550 Hz at stage II, and 280 Hz at stage III). Figure 16 depicts the second mode rotational vibration characteristics. Note that similar conclusions can be reached for the second modal frequencies of 1090, 1610, and 820 Hz, respectively, for stages I to III.

SUMMARY OF RESULTS

This paper presents a vibration analysis with the effects of gearbox motion and mass imbalance for multistage gear transmission. The analysis

combines gear mesh dynamics and structural modal analysis to study the transmission vibrations. The major content of this work can be summarized as follows:

1. A comprehensive approach is developed to combine the nonlinear gear mesh dynamics with structural, lateral, and torsional vibration of the system to determine the global system response.

2. The modal method transforms the equations of motion into modal coordinates to reduce the degrees of freedom of the system of equations.

3. Gear force observations in both the time and frequency domains provide good insights into the source of dominating response forces.

4. The magnitude of the gear mesh force is inversely proportional to the rotor stiffness of the geared system.

5. The influence of the gearbox motion to system vibration is more pronounced in a stiffer rotor system.

6. Gear tooth mesh frequency and torsional modal frequencies have substantial effects on rotational but not on lateral vibrations of the system.

7. Knowledge of modal amplifications under various excitations provide an understanding of the vibrational characteristics of the system. This knowledge is crucial for designing transmissions with improved performance and durability.

REFERENCES

August, R.; and Kasuba, R., "Torsional Vibrations and Dynamic Loads in a Basic Planetary Gear System," Journal of Vibration, Acoustics, Stress, and Reliability in Design, Vol. 108, No. 3, pp. 348-353, 1986.

Boyd, L.S.; and Pike, J.A., "Epicyclic Gear Dynamics," AIAA Paper 87-2042, June 1987. Presented at the AIAA/SAE/ASME/ASEE 23rd Joint Propulsion Conference, San Diego, CA, 1987.

Choy, F.K.; and Li, W., "Frequency Component and Modal Synthesis Analysis of Large Rotor/Bearing Systems with Base Motion Induced Excitations," Journal of Franklin Institute, Vol. 323, No. 2, pp. 145-168, 1987.

Choy, F.K.; Padovan, J.; and Li, W., "Rub in High Performance Turbomachinery: Modelling; Solution Methodology; and Signature Analysis," Mechanical Systems and Signal Processing, Vol. 2, No. 2, pp. 113-133, 1988.

Choy, F.K.; Townsend, D.P.; and Oswald, F.B., "Dynamic Analysis of Multimesh-Gear Helicopter Transmissions," NASA TP-2789, 1988.

Choy, F.K.; Tu, Y.K.; Savage, M.; and Townsend, D.P., "Vibration Signature Analysis of Multistage Gear Transmission," NASA TM-101442, 1989. Presented at the ASME Fifth International Power Transmission and Gearing Conference, Chicago, Illinois, April 1989.

Cornell, R.W., "Compliance and Stress Sensitivity of Spur Gear Teeth," Journal of Mechanical Design, Vol. 103, No. 2, pp. 447-459, 1981.

David, J.W.; and Park, N., "The Vibration Problem In Gear Coupled Rotor Systems," in Rotating Machinery Dynamics; 11th ASME Vibrations and Noise Conference, Boston, MA, Sept. 29, 1987, A. Muszynska and J.C. Simonis, eds., Vol. 2, 1987, pp. 297-304, ASME, New York, 1987.

David, J.W.; Mitchell, L.D.; and Daws, J.W., "Using Transfer Matrices for Parametric System Forced Response," Journal of Vibration, Acoustics, Stress, and Reliability in Design, Vol. 110, No. 3, pp. 263-269, 1988.

Lin, H.; Huston, R.L.; and Coy, J.J., "On Dynamic Loads in Parallel Shaft Transmissions: Part I - Modelling and Analysis," Journal of Mechanisms, Transmissions and Automation in Design, Vol. 110, No. 2, pp. 221-225, 1988.

Mitchell, L.D.; and David, J.W., "Proposed Solution Methodology for the Dynamically Coupled Nonlinear Geared Rotor Mechanics Equations," Journal of Vibration, Stress, and Reliability in Design, Vol. 107, No. 1, pp. 112-116, 1985.

Savage, M.; Caldwell, R.J.; Wisor, J.W.; and Lewicki, D.G., "Gear Mesh Compliance Modelling," NASA TM-88843, 1986. Presented at the Rotary Wing Propulsion System Specialist's Meeting of the American Helicopter Society, Williamsburg, VA, Nov. 12, 1986.

TABLE I. - SYSTEM NATURAL FREQUENCIES

Mode	Stage I	Stage II	Stage III
Torsional natural frequencies, Hz			
1	355	550	280
2	1090	1610	820
Lateral natural frequencies, Hz			
1	115	160	110
2	145	189	200
2	190	264	160

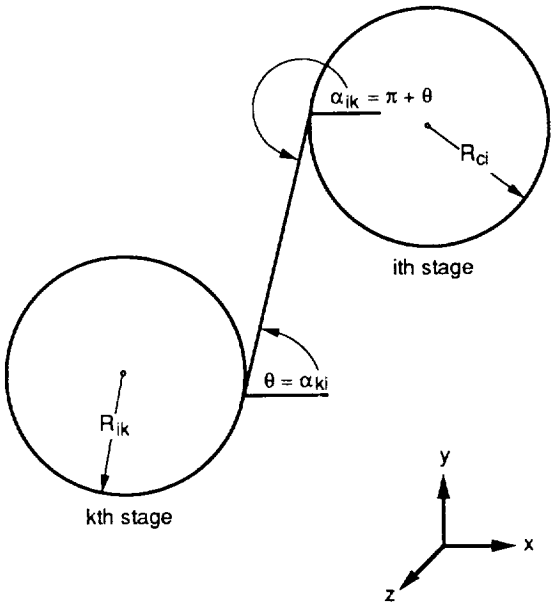

Figure 1.—Coordinate system for gear mesh force.

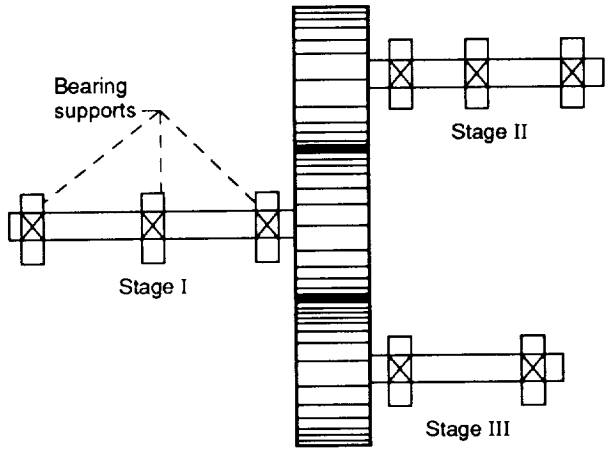

Figure 2.—Three-stage rotor-bearing gear system.

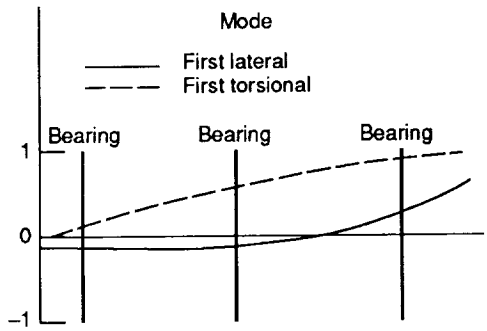

(a) Stage I.

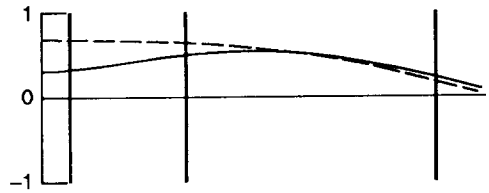

(b) Stage II.

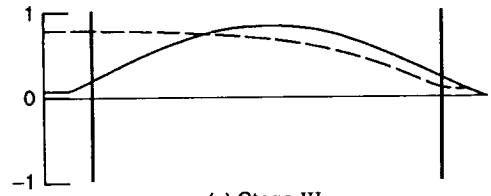

(c) Stage III.

Figure 3.—First vibration mode of three-stage system.

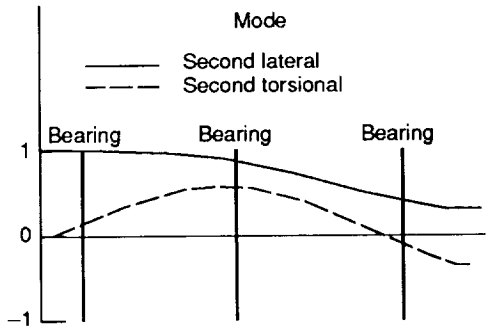

(a) Stage I.

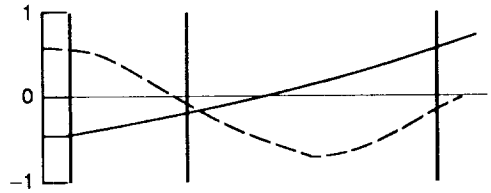

(b) Stage II.

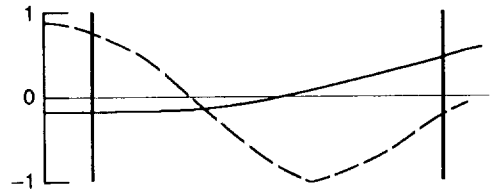

(c) Stage III.

Figure 4.—Second vibration mode of three-stage system.

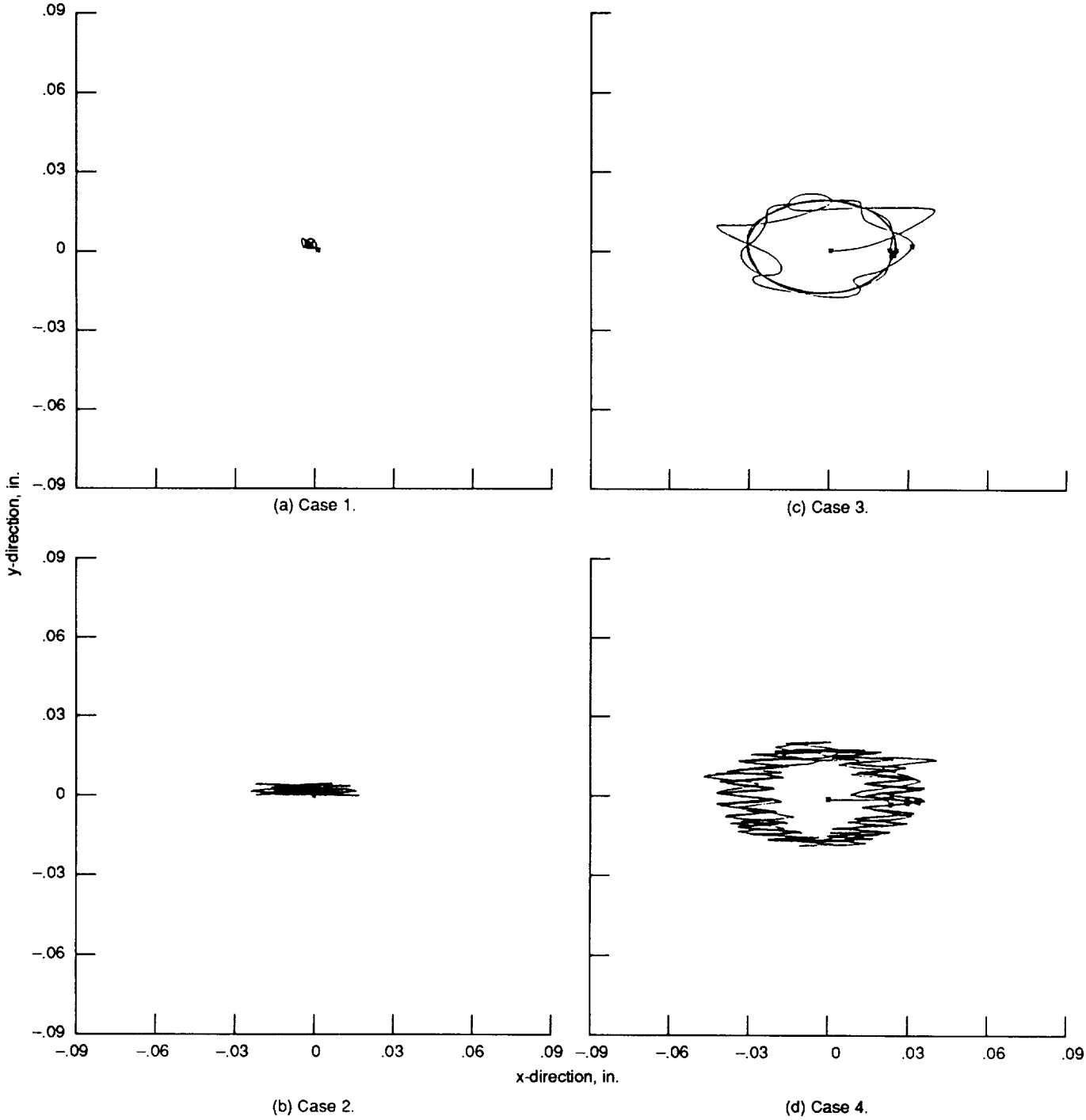

Figure 5.—Stage I rotor vibrational orbit.

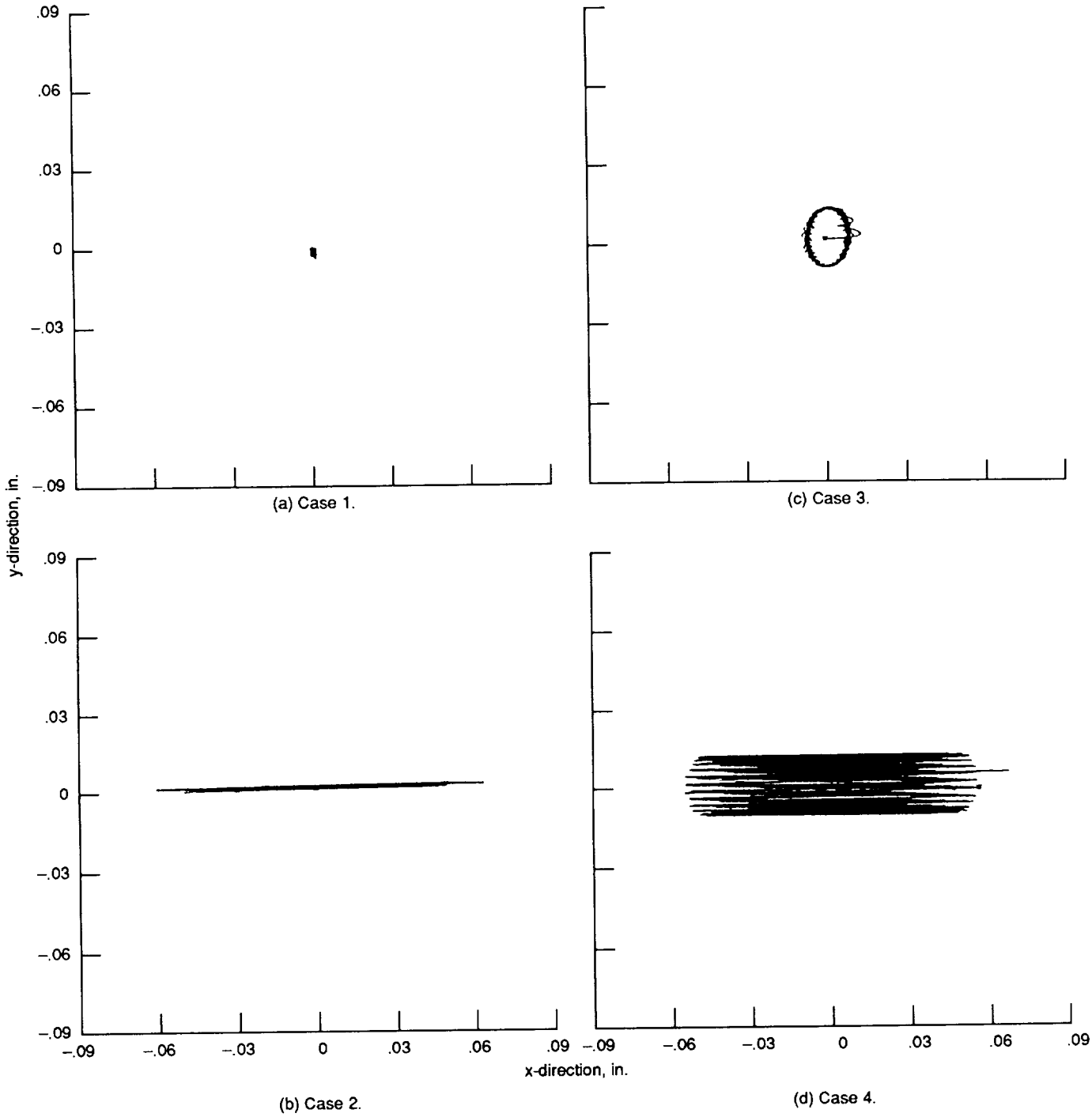

Figure 6.—Stage II rotor vibrational orbit.

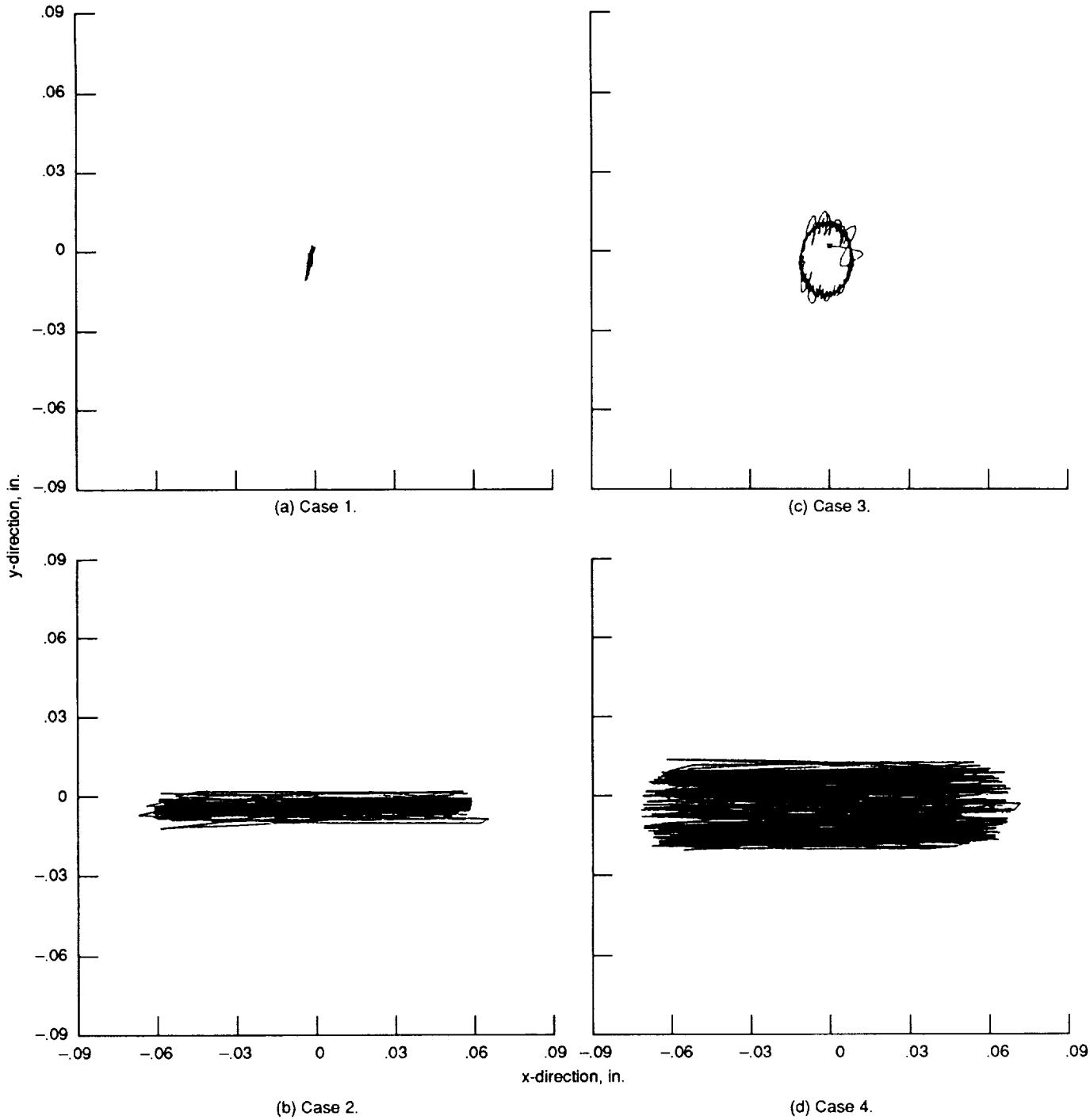

Figure 7.—Stage III rotor vibrational orbit.

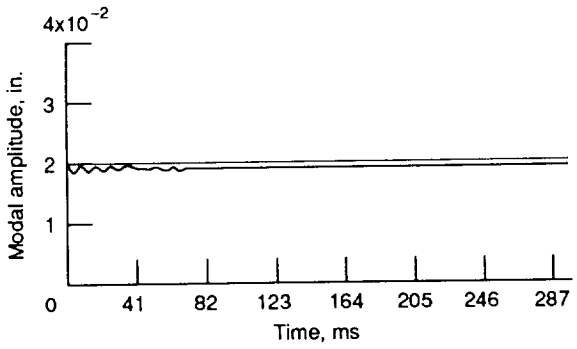

(a) Case 1 in relation to time.

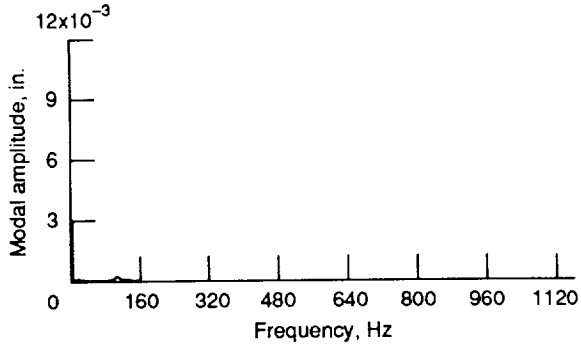

(b) Case 1 in relation to frequency.

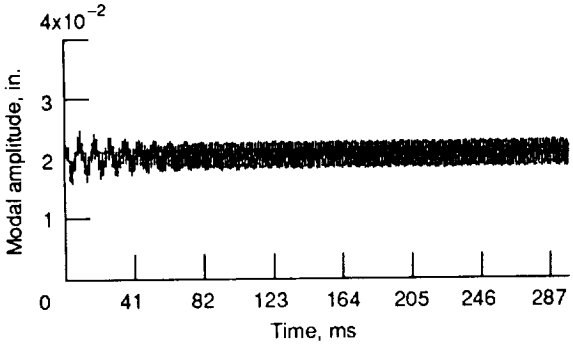

(c) Case 2 in relation to time.

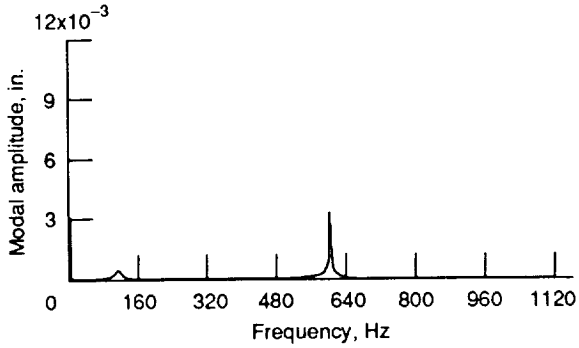

(d) Case 2 in relation to frequency.

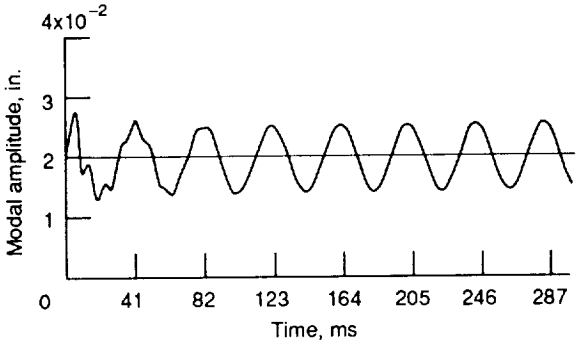

(e) Case 3 in relation to time.

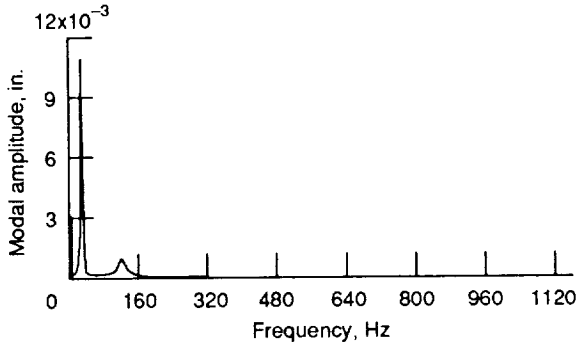

(f) Case 3 in relation to frequency.

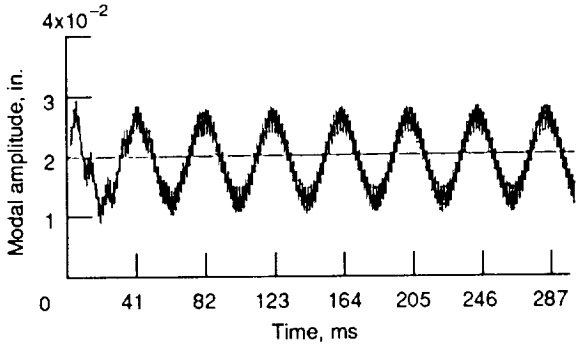

(g) Case 4 in relation to time.

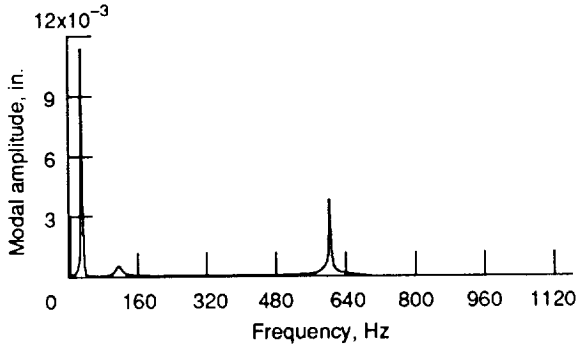

(h) Case 4 in relation to frequency.

Figure 8.—First lateral modal excitation on stage I.

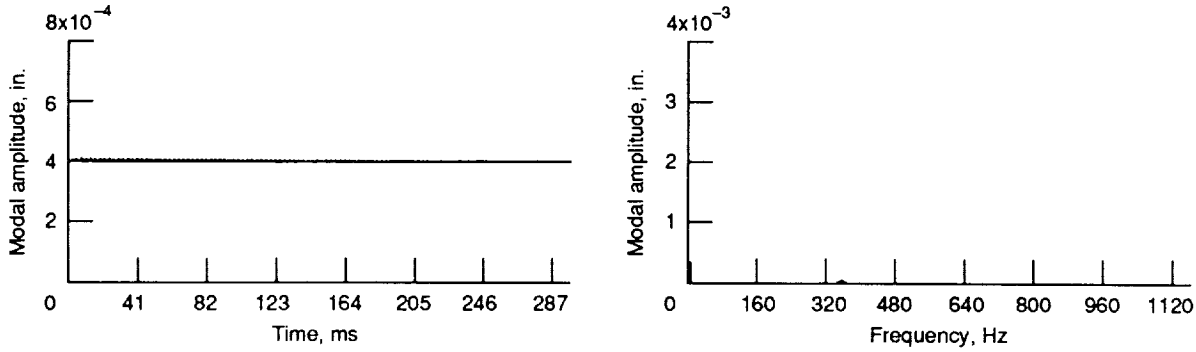

(a) Case 1 in relation to time.

(b) Case 1 in relation to frequency.

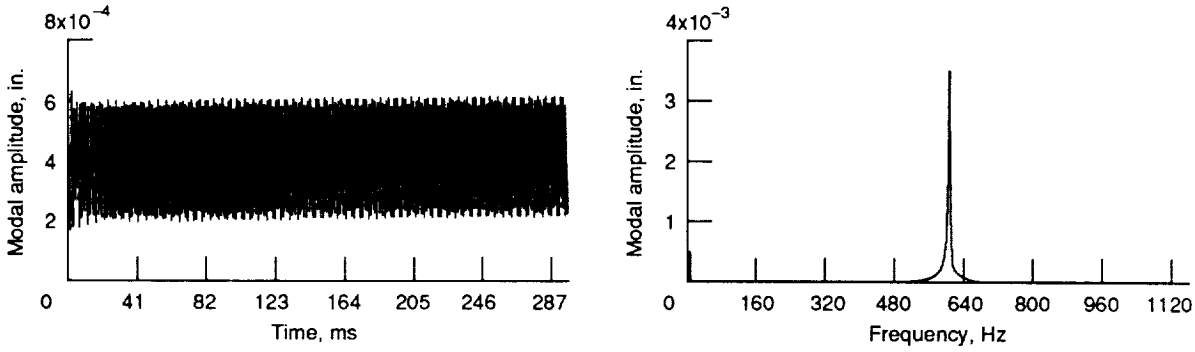

(c) Case 2 in relation to time.

(d) Case 2 in relation to frequency.

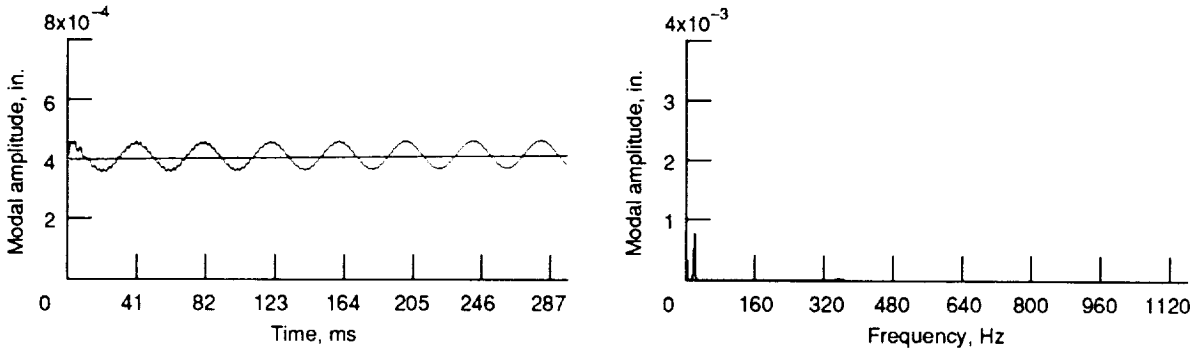

(e) Case 3 in relation to time.

(f) Case 3 in relation to frequency.

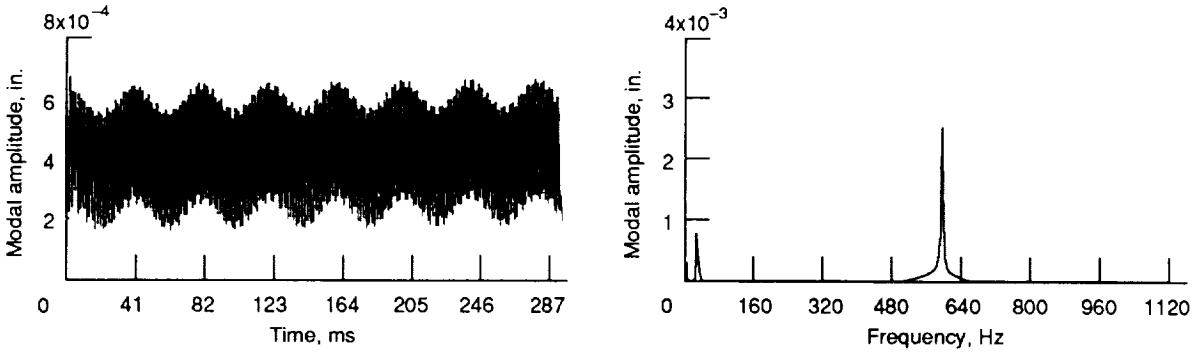

(g) Case 4 in relation to time.

(h) Case 4 in relation to frequency.

Figure 9.—First lateral modal excitation on stage II.

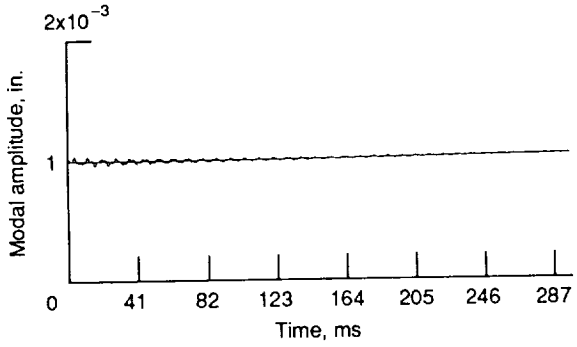

(a) Case 1 in relation to time.

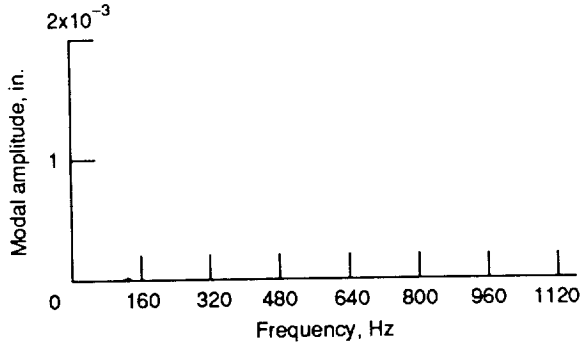

(b) Case 1 in relation to frequency.

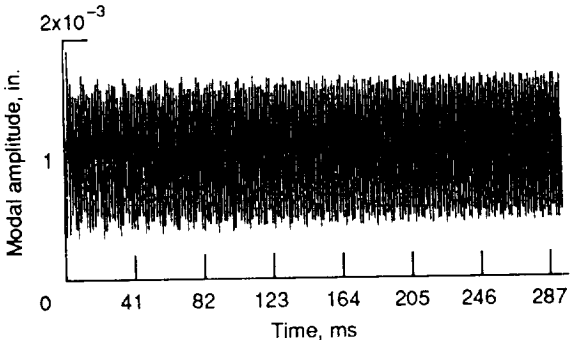

(c) Case 2 in relation to time.

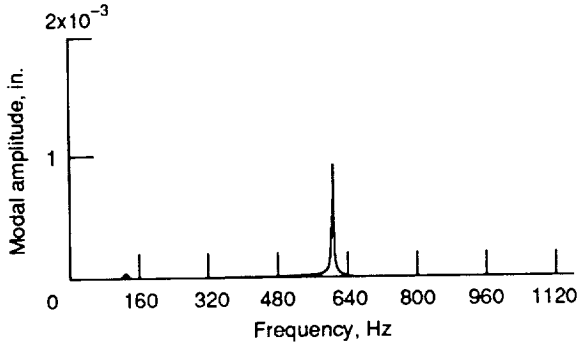

(d) Case 2 in relation to frequency.

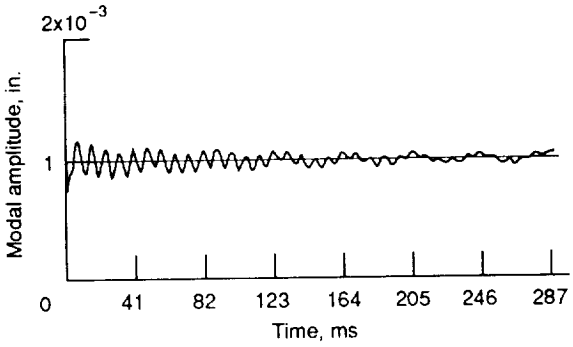

(e) Case 3 in relation to time.

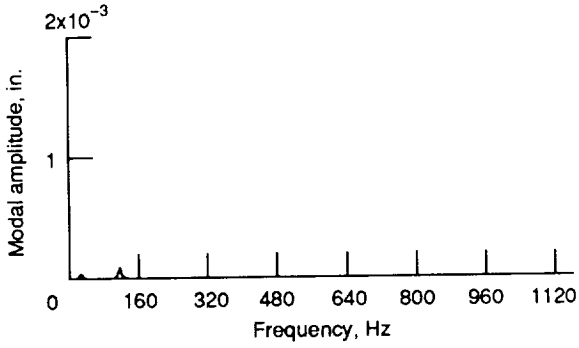

(f) Case 3 in relation to frequency.

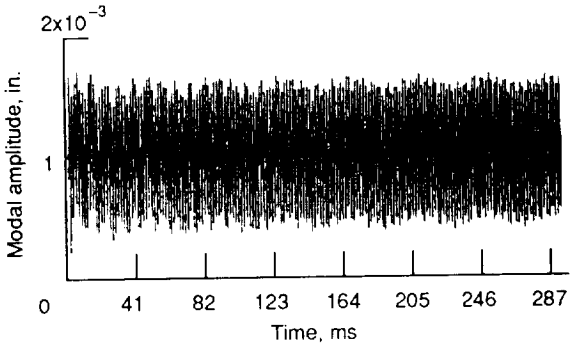

(g) Case 4 in relation to time.

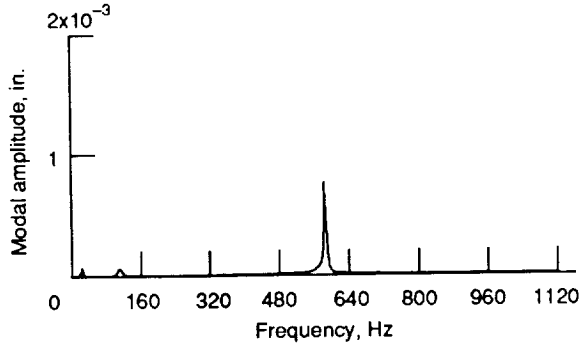

(h) Case 4 in relation to frequency.

Figure 10.—First lateral modal excitation on stage III.

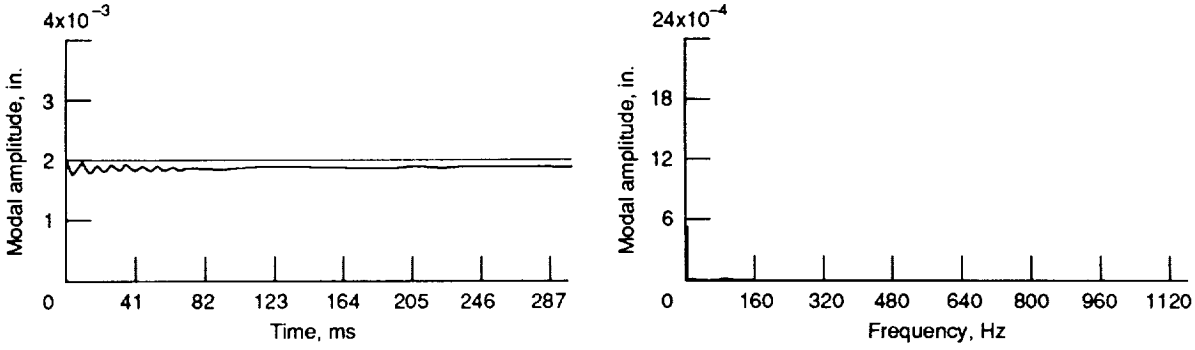

(a) Case 1 in relation to time.

(b) Case 1 in relation to frequency.

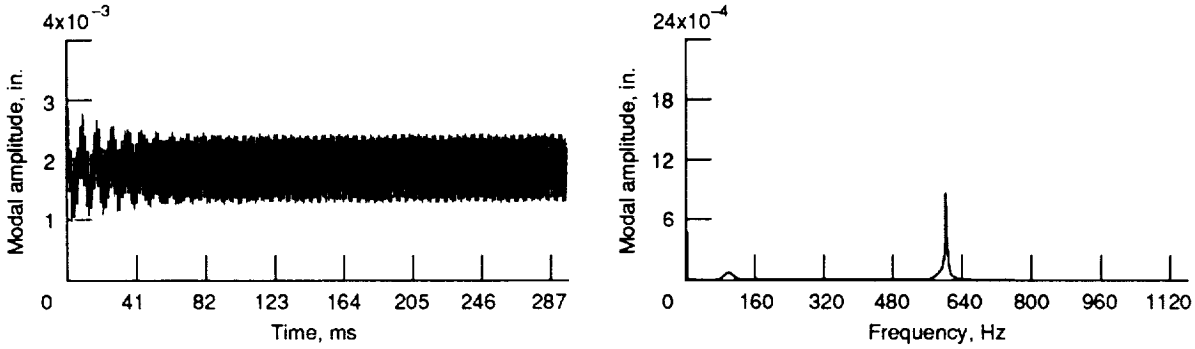

(c) Case 2 in relation to time.

(d) Case 2 in relation to frequency.

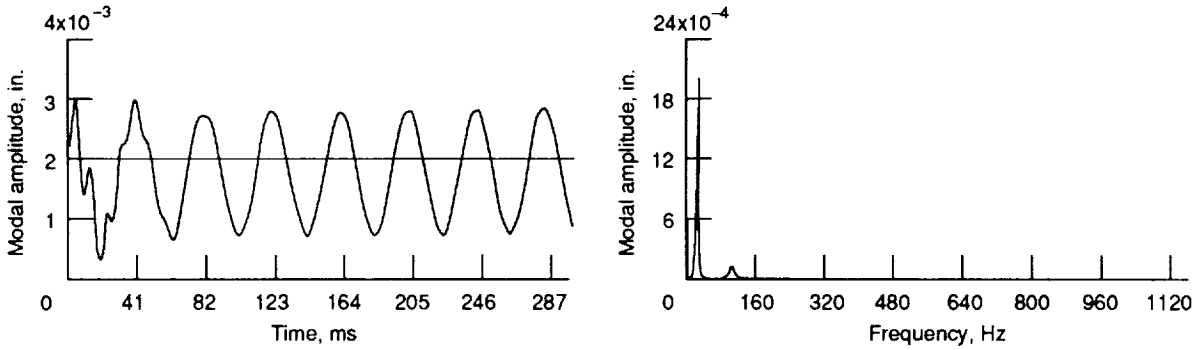

(e) Case 3 in relation to time.

(f) Case 3 in relation to frequency.

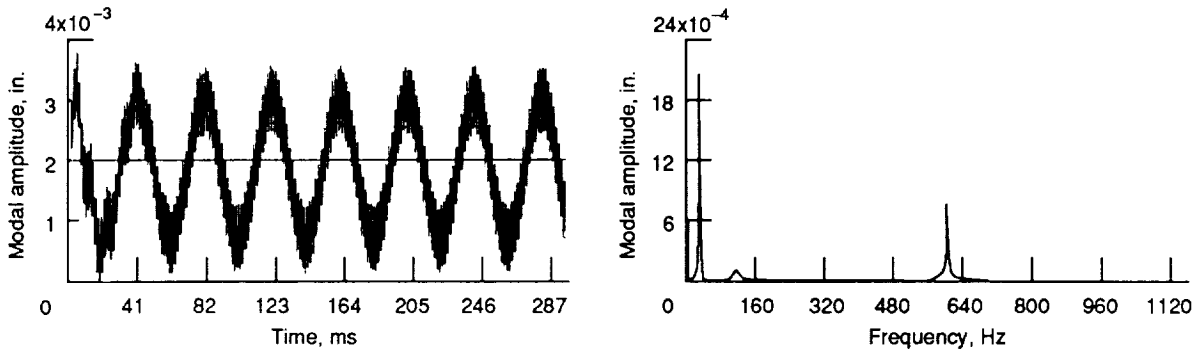

(g) Case 4 in relation to time.

(h) Case 4 in relation to frequency.

Figure 11.—Second lateral modal excitation on stage I.

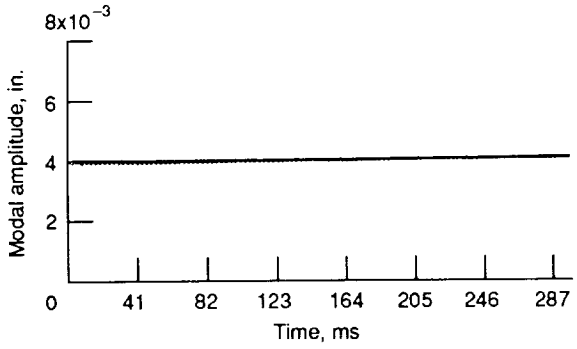

(a) Case 1 in relation to time.

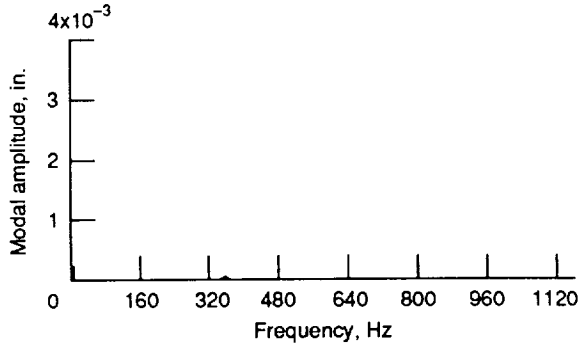

(b) Case 1 in relation to frequency.

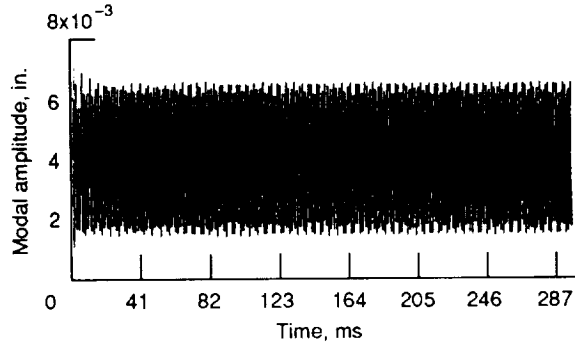

(c) Case 2 in relation to time.

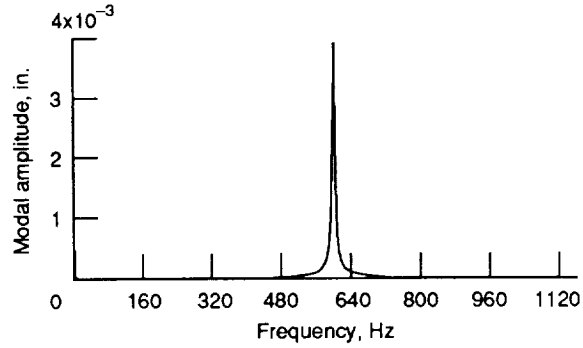

(d) Case 2 in relation to frequency.

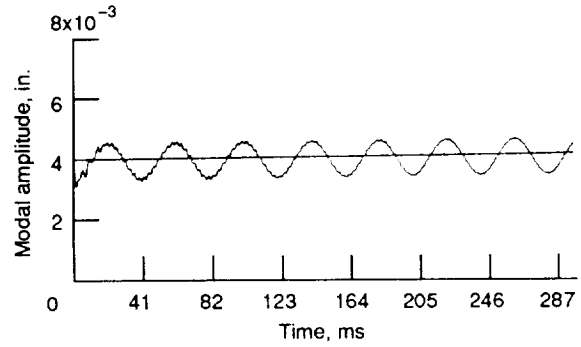

(e) Case 3 in relation to time.

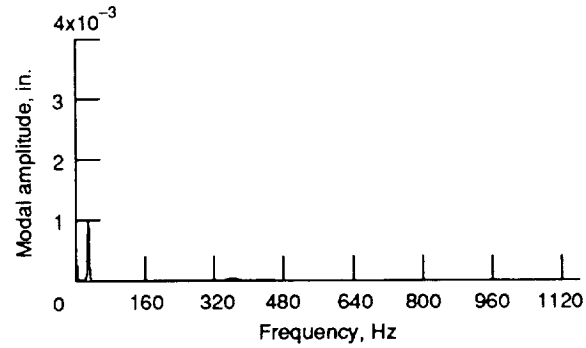

(f) Case 3 in relation to frequency.

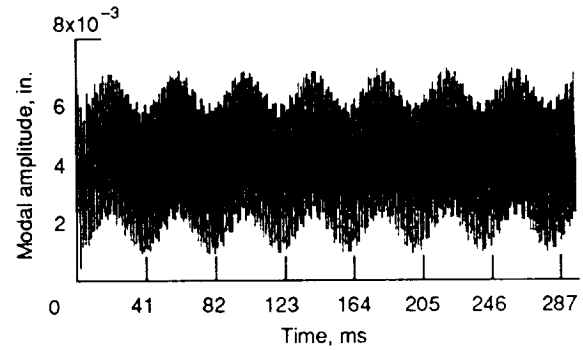

(g) Case 4 in relation to time.

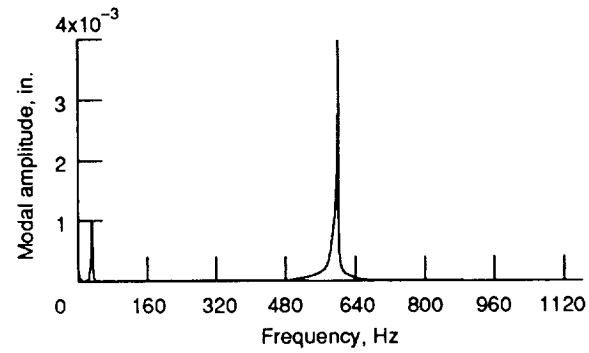

(h) Case 4 in relation to frequency.

Figure 12.—Second lateral modal excitation on stage II.

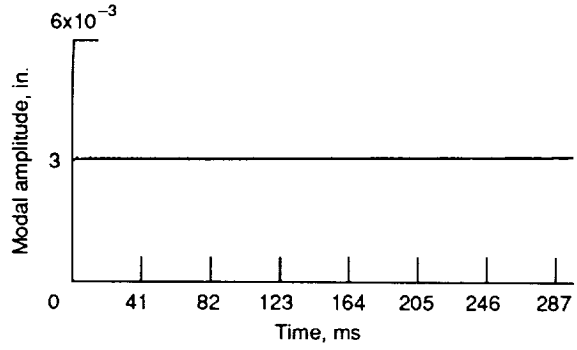

(a) Case 1 in relation to time.

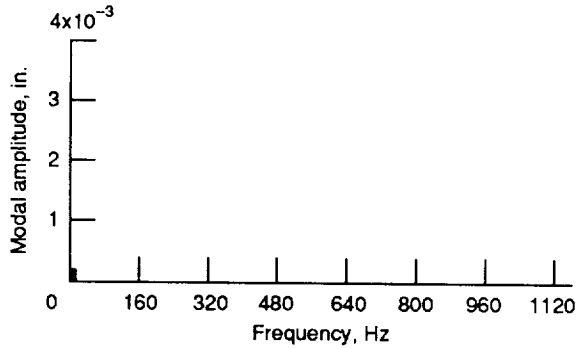

(b) Case 1 in relation to frequency.

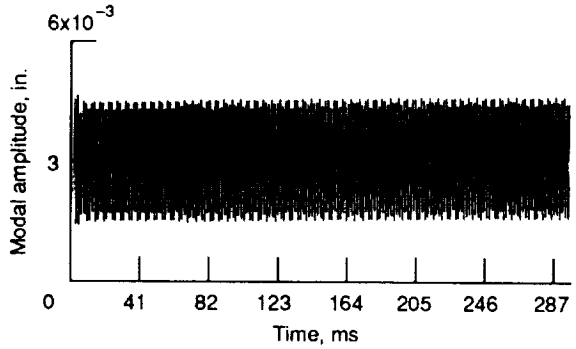

(c) Case 2 in relation to time.

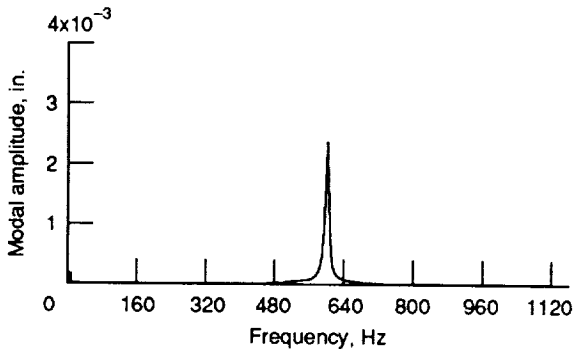

(d) Case 2 in relation to frequency.

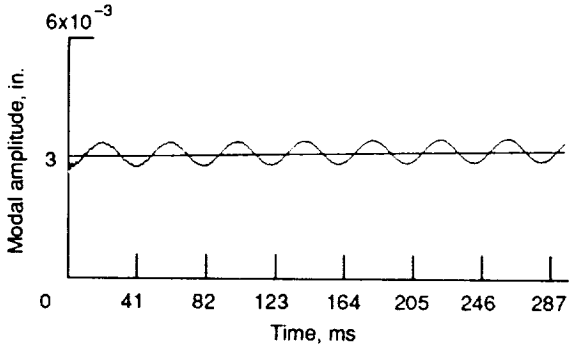

(e) Case 3 in relation to time.

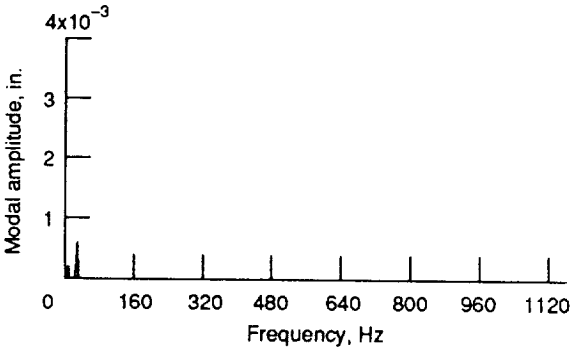

(f) Case 3 in relation to frequency.

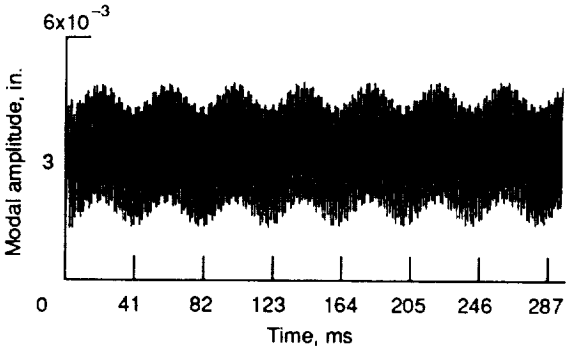

(g) Case 4 in relation to time.

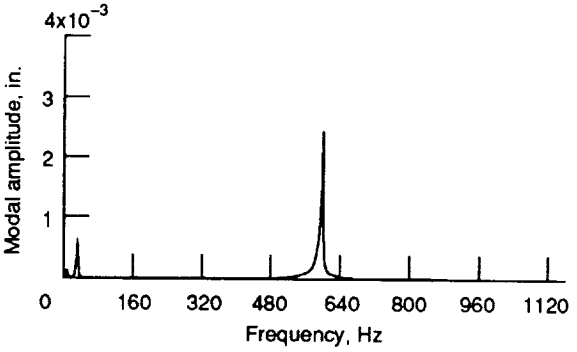

(h) Case 4 in relation to frequency.

Figure 13.—Second lateral modal excitation on stage III.

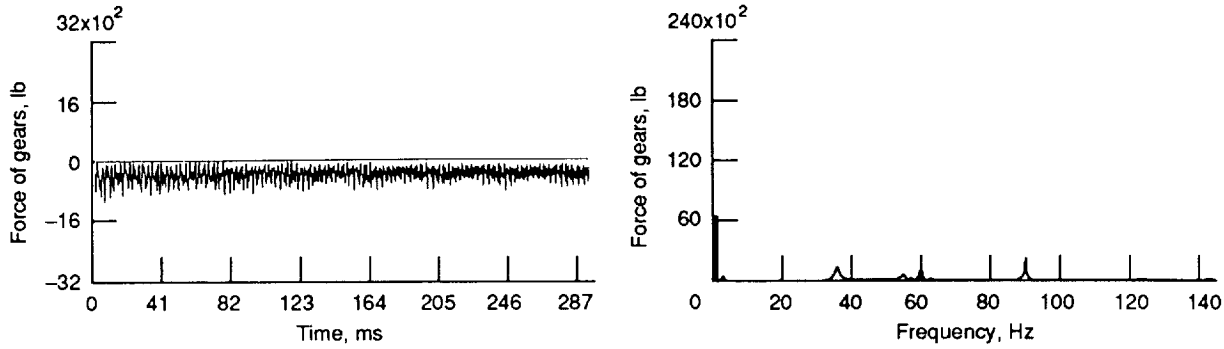

(a) Force of gears 1 and 2 in relation to time.

(b) Force of gears 1 and 2 in relation to frequency.

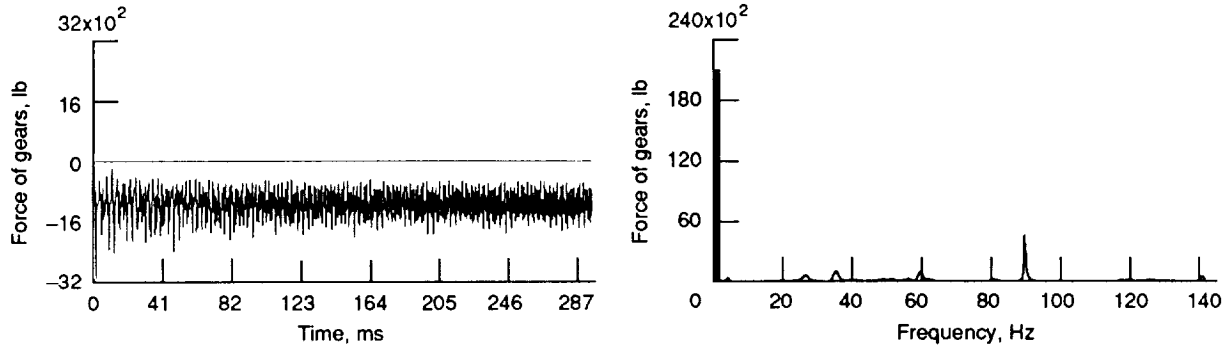

(c) Force of gears 1 and 3 in relation to time.

(d) Force of gears 1 and 3 in relation to frequency.

Figure 14.—Gear force in time and frequency domains.

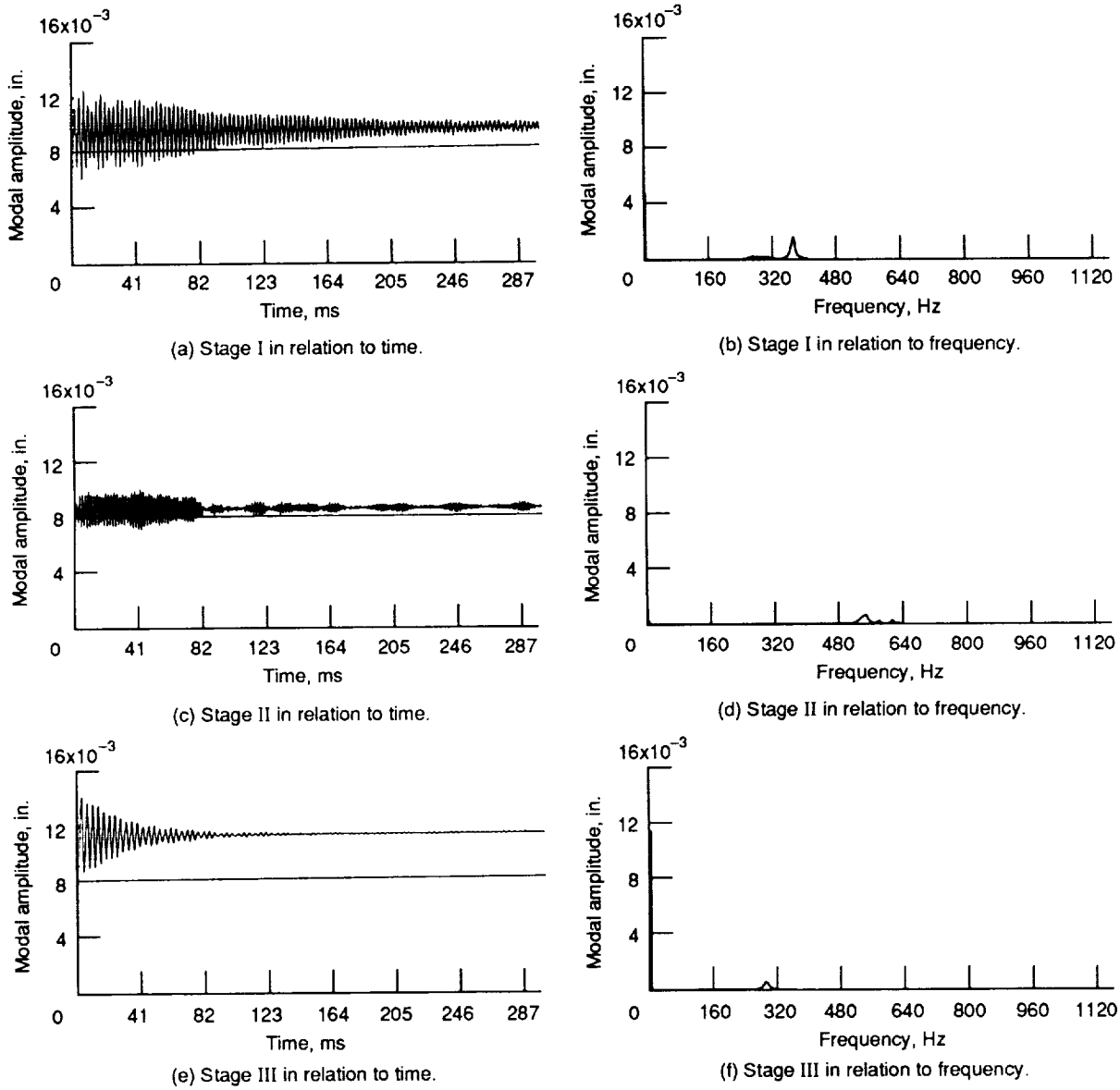

(a) Stage I in relation to time.

(b) Stage I in relation to frequency.

(c) Stage II in relation to time.

(d) Stage II in relation to frequency.

(e) Stage III in relation to time.

(f) Stage III in relation to frequency.

Figure 15.—First torsional modal excitation on stage I.

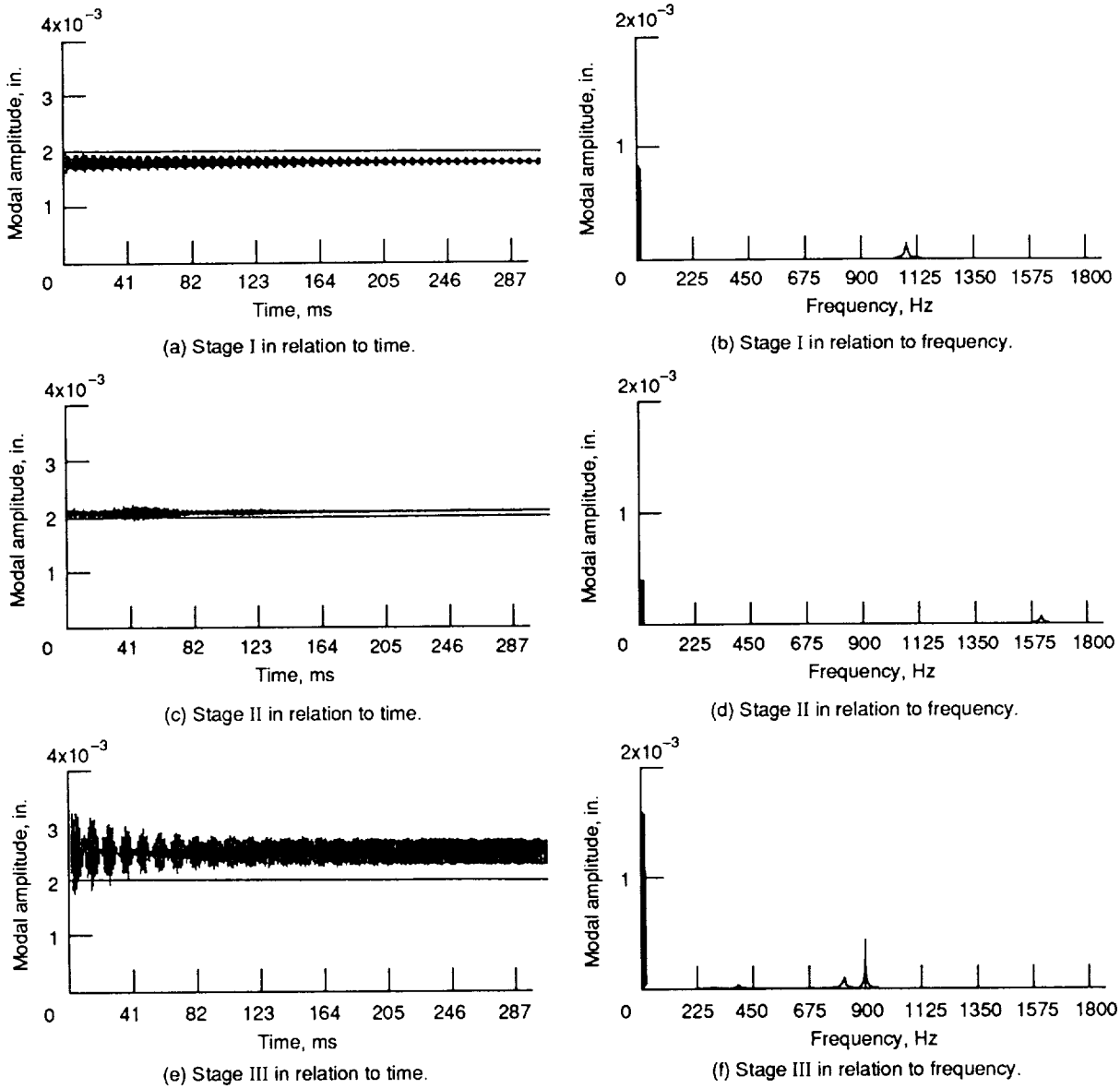

(a) Stage I in relation to time.

(b) Stage I in relation to frequency.

(c) Stage II in relation to time.

(d) Stage II in relation to frequency.

(e) Stage III in relation to time.

(f) Stage III in relation to frequency.

Figure 16.—Second torsional modal excitation on stage I.

NASA
National Aeronautics and Space Administration

Report Documentation Page

1. Report No.	2. Government Accession No.	3. Recipient's Catalog No.
NASA TM-103109 AVSCOM TR 89-C-022		

4. Title and Subtitle	5. Report Date
Dynamics of Multistage Gear Transmission With Effects of Gearbox Vibrations	6. Performing Organization Code

7. Author(s)	8. Performing Organization Report No.
F.K. Choy, Y.K. Tu, J.J. Zakrajsek, and D.P. Townsend	E-5433

9. Performing Organization Name and Address	10. Work Unit No.
NASA Lewis Research Center Cleveland, Ohio 44135-3191 and Propulsion Directorate U.S. Army Aviation Systems Command Cleveland, Ohio 44135-3191	505-63-5A and 505-62-0K 1L162209A47A
	11. Contract or Grant No.
	13. Type of Report and Period Covered Technical Memorandum
12. Sponsoring Agency Name and Address National Aeronautics and Space Administration Washington, D.C. 20546-0001 and U.S. Army Aviation Systems Command St. Louis, Mo. 63120-1798	14. Sponsoring Agency Code

15. Supplementary Notes

Prepared for the CSME Mechanical Engineering Forum 1990 sponsored by the Canadian Society of Mechanical Engineers, Toronto, Canada, June 3-9, 1990, F.K. Choy and Y.K. Tu, Department of Mechanical Engineering, The University of Akron, Akron, Ohio 44325; J.J. Zakrajsek and D.P. Townsend, NASA Lewis Research Center.

16. Abstract

This paper presents a comprehensive approach in analyzing the dynamic behavior of multistage gear transmission systems with the effects of gearbox induced vibrations and mass imbalances of the rotor. The modal method, with undamped frequencies and planar mode shapes, is used to reduce the degrees of freedom of the gear system for time-transient dynamic analysis. Both the lateral and torsional vibration modes of each rotor-bearing-gear stage as well as the interstage vibrational characteristics are coupled together through localized gear mesh tooth interactions. In addition, gearbox vibrations are also coupled to the rotor-bearing-gear system dynamics through bearing support forces between the rotor and the gearbox. Transient and steady state dynamics of lateral and torsional vibrations of the geared system are examined in both time and frequency domains to develop interpretations of the overall modal dynamic characteristics under various operating conditions. A typical three-stage geared system is used as an example. Effects of mass imbalance and gearbox vibrations on the system dynamic behavior are presented in terms of modal excitation functions for both lateral and torsional vibrations. Operational characteristics and conclusions are drawn from the results presented.

17. Key Words (Suggested by Author(s))	18. Distribution Statement
Gearbox Vibration Dynamics Multistage	Unclassified – Unlimited Subject Category 37

19. Security Classif. (of this report)	20. Security Classif. (of this page)	21. No. of pages	22. Price*
Unclassified	Unclassified	24	A03

NASA FORM 1626 OCT 86

*For sale by the National Technical Information Service, Springfield, Virginia 22161